Focusing Effects of L-Dopa in Parkinson's Disease

Bernard Ng,[1]* Samantha Palmer,[2] Rafeef Abugharbieh,[1,3] and Martin J. McKeown[1,2,3,4]

[1]*Biomedical Signal and Image Computing Laboratory, Department of Electrical and Computer Engineering, The University of British Columbia, Vancouver, Canada*
[2]*Pacific Parkinson's Research Center, The University of British Columbia, Vancouver, Canada*
[3]*Brain Research Centre, The University of British Columbia, Vancouver, Canada*
[4]*Department of Medicine (Neurology), The University of British Columbia, Vancouver, Canada*

Abstract: Previous fMRI motor studies in Parkinson's disease (PD) have suggested that L-dopa may "normalize" areas of hypo- and hyperactivity. However, results from these studies, which were largely based on analyzing BOLD signal amplitude, have been conflicting. Examining only amplitude changes at distinct loci may thus be inadequate in fully capturing the activation changes induced by L-dopa. In this article, we extended prior analyses on the effects of L-dopa by investigating both amplitude and spatial changes of brain activation before and after L-dopa. Ten subjects with PD, both on and off medication, and ten healthy, age-matched controls performed a visuo-motor tracking task in which they sinusoidally squeezed a bulb at 0.25, 0.5, and 0.75 Hz. This task was contrasted with static squeezing to generate fMRI activation maps. To investigate the effects of L-dopa, we examined the amplitude and spatial variance of the BOLD response within anatomically-defined regions of interest (ROIs). L-dopa had significant main effects on the amplitude of BOLD signal in bilateral primary motor cortex and left SMA. In contrast, L-dopa-mediated spatial changes were apparent in bilateral cerebellar hemispheres, M1, SMA, and right prefrontal cortex. Moreover, L-dopa appeared to normalize the spatial distribution of ROI activation in PD to that of the controls. Specifically, L-dopa had a "focusing" effect on activity—an effect more pronounced than the typically-measured fMRI amplitude changes. This observation is consistent with modeling studies, which demonstrated that dopamine increases the signal-to-noise ratio at the neuronal level with a resultant focusing of representations at the macroscopic level. *Hum Brain Mapp 31:88–97, 2010.* © 2009 Wiley-Liss, Inc.

Key words: fMRI; spatial analysis; region of interest (ROI); modeling; 3D moment invariants

INTRODUCTION

Despite the clinical benefits of levodopa (L-dopa) on the motor symptoms of Parkinson's disease (PD), neuroimaging studies have revealed conflicting results for the effects of L-dopa on brain activity. Resting state positron emission tomography (PET) studies of PD subjects have shown a pattern of hypermetabolism in lentiform and thalamic areas and hypometabolism of cortical motor regions, which is improved by L-dopa [Eidelberg et al., 1994, 1997; Feigin, 2001]. Earlier studies, however, showed no effect of L-dopa on regional cerebral glucose metabolism [Rougemont et al., 1984]. During voluntary movement, functional magnetic resonance imaging (fMRI) studies have also

*Correspondence to: Bernard Ng, Biomedical Signal and Image Computing Laboratory, Department of Electrical and Computer Engineering, The University of British Columbia (UBC), X421-2366 Main Mall, Vancouver, British Columbia, V6T 1Z4 Canada. E-mail: bernardn@ece.ubc.ca

Received for publication 8 November 2008; Revised 1 June 2009; Accepted 3 June 2009

DOI: 10.1002/hbm.20847

Published online 7 July 2009 in Wiley InterScience (www.interscience.wiley.com).

produced conflicting results. While some have demonstrated hypoactivity of the supplementary motor area (SMA) [Playford et al., 1992], others found increased activity of caudal portions of the SMA [Sabatini et al., 2000]. Similarly, Haslinger et al. [2001] showed hyperactivity of primary motor cortex (M1) while Buhmann et al. [2003] found hypoactivity of M1. Nonetheless, both studies showed that L-dopa "normalized" activity.

A possible explanation of these conflicting results is that the aforementioned studies have focused on examining the amplitude of fMRI BOLD response, and neglected possible characteristic changes in the spatial pattern of activation. Standard approaches, such as statistical parametric mapping (SPM), analyze each voxel in isolation to generate activation maps. Performing group analyses under this voxel-based approach requires spatial normalization to a common template or atlas, which may result in misregistration errors [Castanon et al., 2003], especially for small subcortical regions affected in PD, such as the basal ganglia. Region of interest (ROI)-based techniques, which compare activation in homologous ROIs across subjects without spatial normalization, may overcome some of the difficulties associated with whole-brain warping. However, the optimum way of summarizing the activity within an ROI is unclear. Taking the mean of the activation statistics over an ROI is a simple and popular method [Liu et al., 2002], but neglects important spatial information.

The assumption that only amplitude is modulated by disease or by motor task may be overly simplistic, as accumulating evidence suggests that the spatial distribution of activation, even within an ROI, may also be an important characteristic of brain activity. Thickbroom et al. [1998] have shown in normal subjects that the spatial extent of activation within motor cortex, rather than amplitude of mean response, was modulated by level of force output during a finger flexion task. In PD subjects, a previous study demonstrated that the primary motor cortex contralateral to the affected hand shows fewer active voxels than the cortex contralateral to the unaffected hand, despite the finding that the BOLD signal has no significant difference in peak height [Buhmann et al., 2003]. Moreover, Strafella et al. demonstrated that in PD subjects, the number of voxels showing TMS-induced dopamine release in the putamen was greater in the symptomatic side than the asymptomatic side [Strafella et al., 2005]. Thus, one of the effects of L-dopa may be the "refocusing" of activity in specific regions. This hypothesis can be examined by measuring the spatial extent of activation in the same subjects off and on L-dopa medication.

Traditionally, simple methods that rely on counting the number of active voxels have been used to estimate the spatial extent of activation. However, this metric does not quantify the change in shape, for example whether the activation distribution is focused or diffused, as one can easily imagine a scenario where the same number of voxels is active but the spatial patterns of activation are completely different. To circumvent this limitation, we have recently proposed a method that uses invariant spatial features to characterize the spatial pattern of activation within an ROI [Ng et al., 2006, 2009], while accounting for intersubject variability in size and position. One of the proposed features was specifically designed to measure the spatial extent of activation relative to the center of the ROI activation pattern. We refer to this feature as spatial variance. Using this method, we demonstrated that spatial information can increase the sensitivity to task-related changes in healthy subjects when compared to amplitude information alone [Ng et al., 2006, 2009]. In this study, we applied this method to PD subjects off and on medication and age-matched controls performing a tracking task at three sinusoidal frequencies to investigate the effects of L-dopa. We predict that PD subjects off medication will have a more diffused pattern of ROI activation that normalizes or focuses upon medication.

METHODS

Subjects

The study was approved by the University of British Columbia Ethics Board and all subjects gave written informed consent prior to participating. Ten volunteers with clinically diagnosed PD participated in the study (four men, six women, mean age 66 $\pm$ 8 years, eight right-handed, two left-handed). All subjects had mild to moderate PD (Hoehn and Yahr Stage 2–3) [Hoehn and Yahr, 1967] with mean symptom duration of 5.8 $\pm$ 3 years. All PD subjects were taking L-dopa with an average daily dose of 685 $\pm$ 231 mg. Other medications included ropinirole, bromocriptine, trihexyphenidyl, and domperidone. We also recruited 10 healthy, age-matched control subjects without active neurological disorders (three men, seven women, mean age 57.4 (14 years, nine right-handed, one left-handed) for comparisons. Exclusion criteria included atypical Parkinsonism, presence of other neurological or psychiatric conditions and use of antidepressants, sleeping tablets, or dopamine blocking agents.

Experimental Design

We performed an fMRI experiment involving sinusoidal force production at three frequencies (0.25, 0.5, and 0.75 Hz) to compare the activity among brain regions in PD subjects pre/post medication and age-matched controls. The chosen frequencies were comparable to prior tracking tasks, and we confirmed that this range of frequencies could be accomplished by PD subjects, off-medication in a pilot study. Prior studies that have used a greater range of frequencies typically employed a simpler task such as finger tapping. Faster frequencies of force production using our system were difficult or not possible in both control and PD subjects. By comparing rhythmic force output to static contractions as opposed to rest, we ensured that changes in activity were due to movement frequency and not solely force output per se. The use of a

nonrest comparison condition has also been employed in prior studies. For example, Turner et al. [2003] compared manual tracking to eye tracking only. We note that the frequencies examined for this study were too fast to be directly measured with the sluggish hemodynamic response inherent to the BOLD signal. A block design experiment was thus employed with the task blocks being no longer than 20 s to avoid problems with reduced amplitude of movement secondary to bradykinesia such as digital impedance.

EXPERIMENTAL PROCEDURES

Subjects were asked to lie on their back in the functional magnetic resonance scanner viewing a computer screen via a projection-mirror system. All subjects held in their hand a custom-built MR-compatible rubber squeeze-bulb connected to a pressure transducer outside the scanner room. With their forearm resting down in a stable position, the subjects were instructed to squeeze the bulb using an isometric hand grip and to maintain the same grip throughout the study. Each subject had their maximum voluntary contraction (MVC) measured at the start of the experiment with all subsequent movements scaled to 5–15% of MVC.

Using the squeeze bulb, subjects were required to control the width of an "inflatable ring" displayed as a black horizontal bar on the screen (see Fig. 1). Subjects were instructed to keep this ring within an undulating pathway at all times. Applying greater pressure to the bulb increases the width of the bar and vice versa. To maintain the black bar within the pathway, subjects were required to squeeze at 5–15% MVC. No additional visual feedback or error reporting was given; so subjects had to carefully monitor their own performance. The pathway remained straight (requiring a constant force of 10% of MVC) between sinusoidally-undulating periods of three different frequencies (0.25, 0.5, and 0.75 Hz) presented in pseudo-randomly ordered 19.85-s blocks (exactly 10 TR intervals). An entire run lasted 4 min. All subjects performed the task once with the right hand. Custom Matlab software (Mathworks) and the Psychtoolbox [Brainard, 1997] were used to design and present stimuli, and to collect behavioral data from the response devices.

All PD subjects stopped their anti-Parkinson medications overnight for a minimum of 12 h before the study. Those subjects who were also taking dopamine agonists withdrew from this medication for a minimum of 18 h, and these medications were not administered as part of the study. The mean Unified Parkinson's Disease Rating Scale (UPDRS) motor score during this "off-L-dopa" state was 26 ± 8. No significant correlations between UPDRS motor scores and age were found. All subjects exhibited some aspects of bradykinesia on examination.

After completing the experiment in an off-medication state, subjects were given the equivalent to their usual morning dose of L-dopa (Sinemet CR) in immediate release form (mean 132 ± 29 mg Sinemet IR). They then repeated the same tasks postmedication following a 1-h interval to allow L-dopa to reach peak dose.

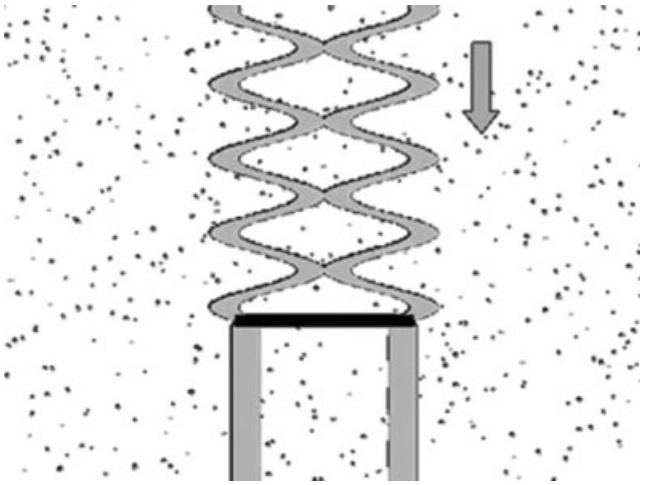

Figure 1.
Experimental task. Subjects were required to squeeze a bulb with sufficient pressure to keep the side of the black bar on the gray path.

Data Acquisition

Functional MRI was collected on a Philips Achieva 3.0 T scanner (Philips, Best, the Netherlands) equipped with a head-coil. T2*-weighted images with blood oxygen level dependent (BOLD) contrast were acquired using an echo-planar (EPI) sequence with a repetition time 1,985 ms, echo time 37 ms, flip angle 90°, field of view (FOV) 240.00 mm, matrix size = 128 × 128, pixel size 1.9 × 1.9 mm^2. Each functional run lasted 4 min. Thirty-six axial slices of 3 mm thickness were collected in each volume, with a gap thickness of 1 mm. We selected slices to cover the dorsal surface of the brain and included the cerebellum ventrally. A high resolution, three-dimensional T1-weighted image consisting of 170 axial slices was acquired of the whole brain to facilitate anatomical localization of activation for each subject.

Head motion was minimized by a foam pillow placed around the subjects head within the coil. Subjects also used ear plugs to minimize the noise of the scanner. The subjects constantly viewed visual stimuli on a screen through a mirror built into the head coil.

fMRI Data Preprocessing and Analysis

The functional MRI data were preprocessed for each subject using Brain Voyager's (Brain Innovation B.V.) trilinear interpolation for 3D motion correction and sinc interpolation for slice time correction. The data were then further motion corrected with MCICA, a computationally

expensive but highly accurate method for motion correction [Liao et al., 2005]. No temporal smoothing, spatial smoothing, or spatial normalization was performed. To coregister the anatomical and functional images, the Brain Extraction Tool (BET) in MRIcro [Rorden and Brett, 2000] was used to strip the skull off of the anatomical and first functional image from each run to enable a more accurate alignment of the functional and anatomical scans. Custom scripts in Amira software (Mercury Computer Systems, San Diego, USA) were then used to coregister the anatomical and functional images. Sixteen specific ROIs were manually drawn on each aligned structural scan based upon anatomical landmarks and guided by a neurological atlas [Talairach and Tournoux, 1988] using the Amira software. ROIs included: primary motor cortex (M1) (Brodmann Area 4), supplementary motor cortex (SMA) (Brodmann Area 6), prefrontal cortex (PFC) (Brodmann Area 9 and 10), caudate (CAU), putamen (PUT), thalamus (THA), cerebellum (CER), and anterior cingulate cortex (ACC) (Brodmann Area 28 and 32). The labels on the segmented anatomical scans were resliced to isotropic voxels at the fMRI resolution of $3 \times 3 \times 3$ mm^3. The raw time courses of the voxels within each ROI were then extracted. A hybrid Independent Component Analysis (ICA)/General Linear Model scheme was used to contrast each of the three frequency blocks with the static force condition [McKeown, 2000] to create statistical parametric maps for each ROI.

To characterize the spatial distribution changes of activation statistics within each ROI, we used an invariant moment-based feature that we previously proposed [Ng et al., 2006, 2009] to measure the spatial variance of ROI activation (see Appendix). To decouple the effects of amplitude, we normalized the activation statistics to the range of [0,1]. Previous studies have also characterized ROI activity by measuring the spatial extent of activation but only with the percentage of activated voxels, which do not incorporate the spatial characteristics of the activation distribution. Instead, our feature measures the spread of activation relative to the activation centroid, which in effect distinguishes whether an ROI activation pattern is focused or diffused. For comparison, we also thresholded the t-statistics of BOLD signal changes at 1.96, and computed the mean t-statistic within each ROI under the different task conditions. A 2×3 repeated-measures designed ANOVA was performed on the PD data to analyze the main effects of medication, movement frequency, and any interactions between these two factors. Also, a paired-test was performed to examine the effects of medication at each task frequency. A threshold corresponding to an uncorrected P value of 0.05 with false discovery rate (FDR) correction was used to detect significance. For the omnibus test, we listed the F values, instead of the P values, to facilitate direct comparisons of effect sizes between amplitude and spatial variance. For the frequency-specific contrasts, we provided the (signed) t values for analyzing the direction of changes in amplitude and spatial variance.

In ROIs where a significant main effect of medication for both amplitude and spatial variance were present, we compared the spatial variance of ROI activation in PD patients with that of normal subjects who did not receive any medication to determine whether L-dopa normalizes the activity of PD. In addition, we plotted the ROI activation t-statistics before and after medication to visually demonstrate how the spatial distribution of activation was altered by L-dopa. To ensure that the detected activation differences between controls and PD off and on medication were not due to differences in task performance, we calculated the performance error of each subject at each frequency, and applied an ANOVA to the error rates. Error was computed as the distance between the squeeze-bulb-controlled bar and the target pathway normalized by the width of the pathway. In addition, we compared the error rates of the first and second block of each frequency to confirm that no significant fatigue or practice effects were present within a session at the behavioral level. We have also examined potential fatigue and practice effects within a session at the brain activity level by first splitting the voxel intensity time courses into two halves and estimating the activation effects of each half using a general linear model (GLM). We then computed the spatial variance using the activation effects of each half and applied a paired t test. An uncorrected threshold of $P < 0.05$ was used.

RESULTS

Behavioral Data

Figure 2 shows a summary of the behavioral data, demonstrating that the performance of controls and PD off and on medication were similar. Peaks in the frequency spectra of the squeeze output correctly corresponded to the target frequency of each task block. Applying an ANOVA on the performance error rates detected no significant differences between any of the subject groups ($F(2,166) = 1.56$, $P = 0.2132$). Comparison of error rates for the first and second block of each frequency did not demonstrate significant practice effects within a session ($F(1,345) = 1.53$, $P = 0.2171$).

Amplitude of BOLD Signal Changes

Applying an ANOVA on the activation amplitude demonstrated that bilateral motor cortices and the contralateral SMA were significantly affected by L-dopa medication (Table I). Frequency had a main effect in left putamen, bilateral M1, and bilateral SMA. Assessing the effects of L-dopa on the mean t-statistics at each frequency individually detected no significant changes within any ROIs at the slow frequency (Table I). At the medium frequency, only the left primary cortex demonstrated a significant decrease. At the fastest frequency, significant decreases were detected in the contralateral SMA and ipsilateral putamen, thalamus, cerebellum, and primary cortex.

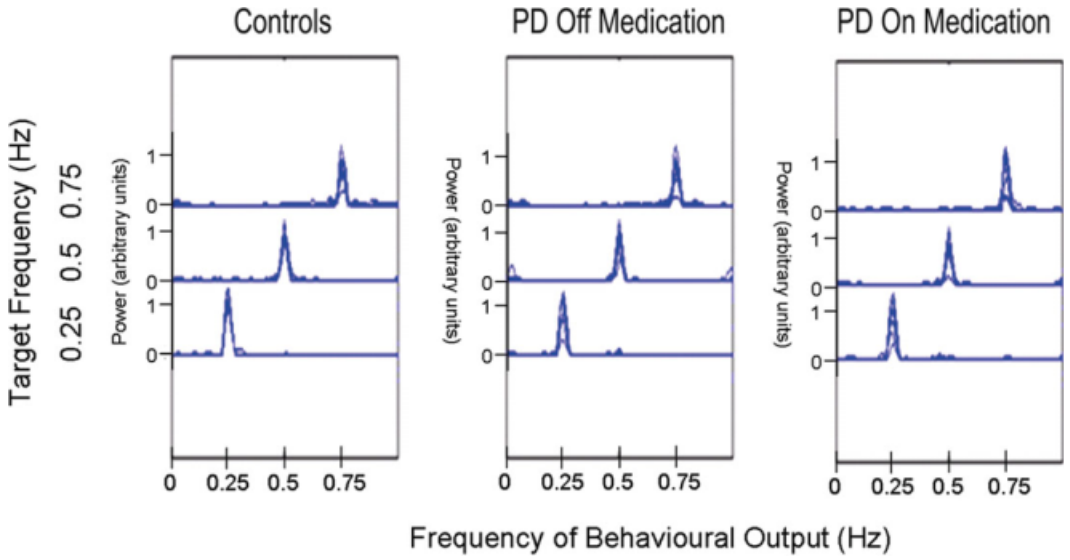

Figure 2.

Summary of the behavioral data. Power spectrum of the behavioral output for each subject is overlaid with each of the three task frequencies displayed as a separate curve. The frequencies at which the power spectrum of the squeeze output peaked correspond to the target frequencies. Task performance of controls and PD off and on medication were similar with no significant group differences detected in the error rates ($F(2,166) = 1.56$, $P = 0.2132$). [Color figure can be viewed in the online issue, which is available at www.interscience.wiley.com.]

Spatial Variance of Activation

Significant main effects of medication were detected in bilateral cerebellar hemispheres, bilateral primary motor cortices, bilateral SMA, and ipsilateral prefrontal cortex. A significant interaction in the left prefrontal cortex was found (Table II). No main effect of frequency was detected, but frequency-specific effects of L-dopa on spatial variance were found in the ipsilateral cerebellum and SMA, and contralateral primary motor cortex at the slow frequency. At medium frequency, significant medication effects were detected in the contralateral thalamus, ipsilateral cerebellum, and bilateral primary motor and supplementary motor cortices. At the highest frequency,

TABLE I. Significant levels for changes in amplitude

	Omnibus F values			PD pre vs. post (signed) t values		
	Drug (df = 1 × 9)	Freq (df = 2 × 9)	Drugxfreq (df = 2 × 18)	Slow (df = 9)	Med (df = 9)	Fast (df = 9)
LPUT	0.673	**8.8408***	0.9731	0.0387	0.3577	2.2117
RPUT	3.005	1.3327	0.9617	0.8733	0.8279	**3.5048***
LCAU	0.0204	0.6264	1.2633	0.2186	−1.8418	0.4649
RCAU	0.5681	0.9952	1.8381	0.1279	−0.9090	1.5609
LTHA	3.2017	2.2485	0.5614	0.5350	1.2289	1.9743
RTHA	6.3626	0.8866	0.8143	1.0246	1.3428	**2.7468***
LCER	4.2957	3.9746	1.8672	0.3238	1.7032	2.4203
RCER	6.7006	3.7269	1.9682	0.7144	1.6627	**2.7120***
LM1	**14.8849***	**6.5018***	0.1797	1.9013	**3.1898***	2.1657
RM1	**10.3895***	**7.0887***	0.7666	1.9949	1.8447	**3.0737***
LSMA	**7.5348***	**4.9269***	2.3465	0.6627	1.5783	**3.3468***
RSMA	5.6209	**5.9822***	1.076	1.8681	1.0667	2.4745
LPFC	1.6699	1.351	0.9966	1.2107	0.0048	1.9988
RPFC	2.1181	2.2402	0.6813	1.0585	0.4431	2.2878
LACC	1.6492	0.1546	1.5574	1.0295	−0.6637	1.5231
RACC	2.1335	1.4331	1.7187	1.3674	0.3025	1.9277

Levels that are significant for a P value <0.05 with FDR correction ($P < 0.026$) are highlighted in bold*. df = degrees of freedom.

TABLE II. Significant levels for changes in spatial variance

	Omnibus F values			PD pre vs. post (signed) t values		
	Drug (df = 1 × 9)	Freq (df = 2 × 9)	Drugxfreq (df = 2 × 18)	Slow (df = 9)	Med (df = 9)	Fast (df = 9)
LPUT	6.5223	2.0291	2.1145	1.0635	1.5567	2.2143
RPUT	0.7215	2.9808	0.7837	1.1852	−0.2336	0.8348
LCAU	0.7839	2.4848	0.5714	1.4493	0.1426	0.4231
RCAU	1.3244	0.5395	0.0049	0.9300	0.9067	0.6653
LTHA	5.6095	1.7118	0.8005	1.8939	**2.7875***	1.7908
RTHA	3.7745	3.348	0.132	1.7606	1.6623	1.8535
LCER	**16.3948***	4.431	0.0733	2.2859	2.5362	**3.4764***
RCER	**14.7629***	4.4819	1.1506	**3.0916***	**4.0051***	2.4414
LM1	**21.1873***	2.1283	0.1104	**4.6332***	**3.7173***	2.3194
RM1	**15.9926***	3.2057	0.9148	2.0983	**3.8733***	**5.5411***
LSMA	**17.6862***	2.02	0.6574	2.2920	**2.7982***	**3.6637***
RSMA	**22.0431***	4.2877	0.4216	**3.5140***	**3.2640***	**3.1688***
LPFC	5.2297	0.303	**4.7305***	0.1934	1.0652	**3.5769***
RPFC	**8.8842***	3.0336	2.6654	1.5191	0.4227	**3.2107***
LACC	0.3014	0.3971	2.2213	1.5437	−1.0503	0.4792
RACC	1.6947	0.5357	0.929	1.4865	0.0150	1.0911

Levels that are significant for a P value <0.05 with FDR correction ($P < 0.026$) are highlighted in bold*. df = degrees of freedom.

significant effects were detected in bilateral prefrontal and supplementary motor cortices, as well as contralateral cerebellum and ipsilateral primary motor cortex.

Normalization by L-Dopa

Figure 3 shows a plot of the t-statistics within the right M1 of an exemplar PD subject off and on L-dopa. Comparing the spatial distribution of t-statistics, L-dopa appears to "refocus" the area of activation. In fact, the signs of the t values in Table II indicate that L-dopa refocuses the activation distributions in all detected ROIs. This trend was consistently found in all PD subjects as shown in Figure 4, where the spatial variance of activation in PD subjects off and on medication as compared to healthy age-matched controls within the left SMA and right M1 (two regions where both amplitude and spatial distribution of activation was significantly affected by L-dopa) are plotted. The spatial variance of activation within these two regions was reduced to a similar level as controls upon medication, thus demonstrating the normalizing effect of L-dopa. To test for potential practice and fatigue effects in brain activation, we applied a t test to the spatial variance estimated from the two halves of the voxel intensity time courses. No significant effects of practice or fatigue were observed within a session (see Fig. 5).

DISCUSSION

A predominant effect of L-dopa appears to be a change in the spatial extent of activation in both cortical and subcortical regions. In fact, the spatial effects of medication were significant in the contralateral motor cortex and ipsilateral cerebellum even at the lowest frequency, whereas medication-related changes in amplitude, as estimated with mean t-statistics, were only evident at the higher frequencies, thus demonstrating the importance of

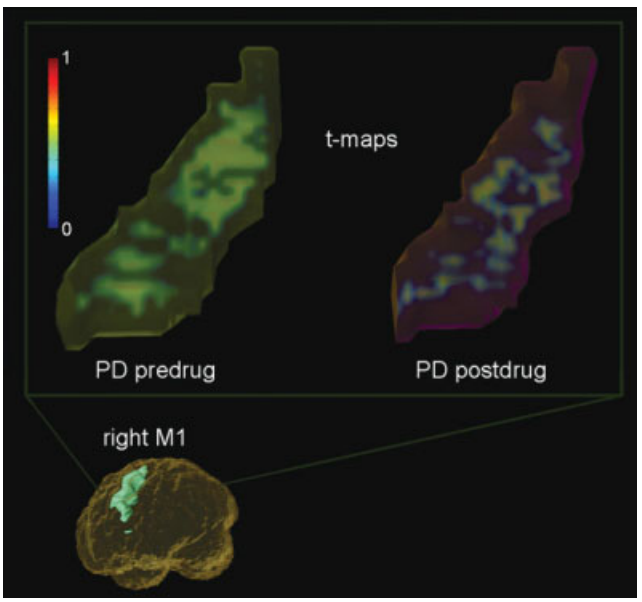

Figure 3.
Focusing effect of L-dopa seen in a typical PD subject. The t-maps shown (right M1) include all voxels with positive t values normalized between [0,1] to emphasize the spatial distribution changes. (top left) A much wider recruitment of the ROI was required to perform the same motor task prior to medication. (top right) The ROI activation pattern appears to focus upon medication. [Color figure can be viewed in the online issue, which is available at www.interscience.wiley.com.]

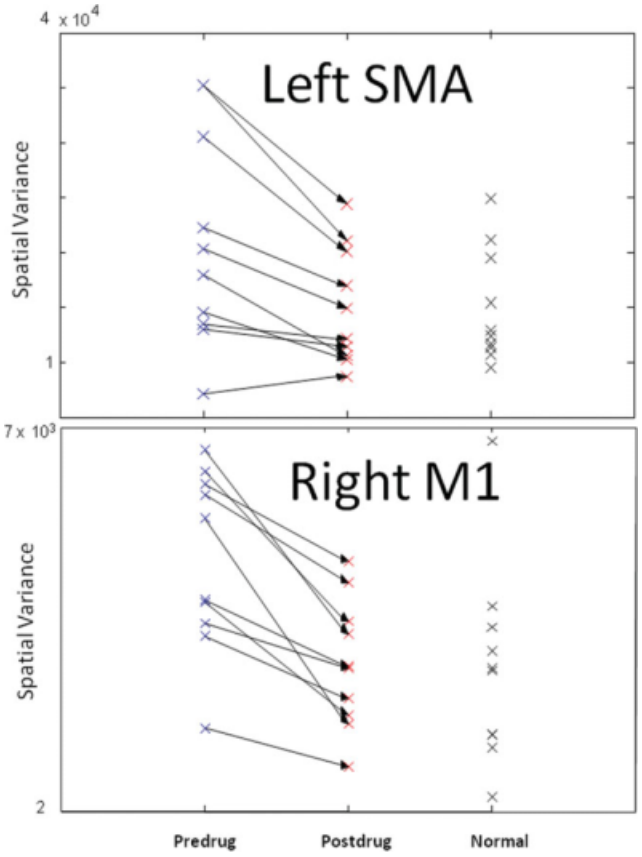

Figure 4.

Normalization of the spatial variance of activation within an ROI by L-dopa. (top panel) The spatial variance of a region demonstrating a significant effect of L-dopa (the left SMA) is plotted. The arrows represent the effects of L-dopa on the spatial variance of each PD subject. The feature values for the normal subjects are shown for comparison. (bottom panel) Normalization of spatial variance in a region ipsilateral to the movement (right primary motor cortex, M1). L-dopa appears to refocus the activation of M1 in PD with the resultant spatial extent becoming more similar to that of the controls. [Color figure can be viewed in the online issue, which is available at www.interscience.wiley.com.]

incorporating spatial information. Also, the ANOVA results demonstrate that the effected sizes of spatial variance were larger than that of amplitude for all ROIs displaying significant L-dopa effects on both features. Nevertheless, for a few of the ROIs during the highest frequency task, medication-related changes were only present in the activation amplitude, thus integrating amplitude and spatial variance to more fully characterized activation changes would be desirable.

Our finding of the wider spread of activation in PD subjects off-medication is consistent with prior cognitive studies, where increase in activation amplitude and spatial extent (by voxel counts) were found in the prefrontal cortex [Monchi et al., 2004]. The focusing effect of L-dopa observed in the current study is also consistent with cognitive studies, where L-dopa was shown to reduce the regional cerebral blood flow (rCBF) in the prefrontal cortex during a working memory task [Cools et al., 2002]. Similar findings were observed in a working memory study by Mattay et al. [2002] and similar effects were seen in healthy controls given methylphenidate [Mehta et al., 2000].

The observed focusing effect likely resulted from the dopamine-induced increase in signal-to-noise in the cortical microcircuits [Winterer et al., 2006], which manifests in the BOLD activation as a sharpening or focusing of response. In computational modeling studies, the effects of dopamine at the individual neuronal level are often modeled as a change in shape of the normally sigmoid curve that relates neuronal inputs to output firing rates. Increasing dopamine results in a more nonlinear curve approaching a threshold-like function, while decreasing dopamine results in the input–output curve becoming more linear [Sikstrom, 2007]. Neurons with threshold-like functions are less sensitive to small synaptic fluctuations that would be seen with more linear regimes, and thus dopamine can be considered as increasing the signal-to-noise of the neuron. When the effects on individual neuronal units are assembled into a network, the macroscopic effect is that the low-dopamine states, as would be seen in PD, result in indistinct neural representations with many units having similar representations, as opposed to a few selected units being active when the modeled dopamine levels are higher [Li and Sikstrom, 2002; Sikstrom, 2007]. Also, studies of COMT (catechol-*O*-methyltransferase) genotype (which codes for the dopamine catabolising enzyme COMT) showed relatively diminished BOLD response and increased noise in COMT-Val carriers (which have lower levels of available synaptic dopamine) [Winterer et al., 2006]. Thus, the focusing effect of dopamine observed in the current motor experiment conforms to results in other domains.

An alternative explanation for the observed changes in spatial distribution relates to the vascular effect of dopamine, which affects BOLD signal changes by altering local blood flow. This explanation, however, seems unlikely given the results in previous studies where L-dopa was found to increase rCBF in some areas and decreased rCBF in others [Cools et al., 2002], whereas L-dopa only decreased spatial variance in a subset of ROIs in the present study. Another important consideration is the potential effect of motor learning on the extent of activation. Karni et al. [1995] have shown changes in the spatial extent (by voxel counts) of activity with practice, both within and between training sessions. These effects were complex, with order effects predominant in early training sessions, regardless of whether the sequence was trained or untrained. However, in later sessions, when performance had reached an asymptotic level, the trained sequence produced a consistently larger spatial extent of activation compared to a control sequence made up of the same submovements. Since we only observed a decrease in spatial

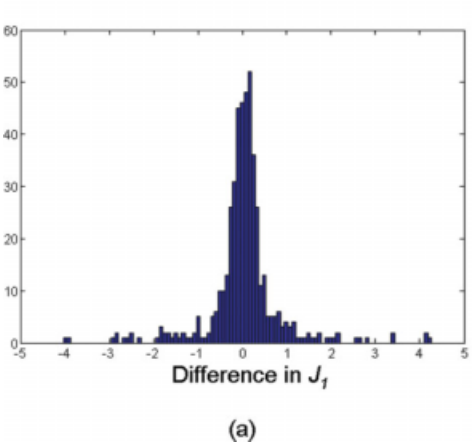

	Controls	PD predrug	PD postdrug
LPUT	0.7617	0.5573	0.7441
RPUT	0.7156	0.5755	0.8460
LCAU	0.3052	0.3298	0.4688
RCAU	0.5527	0.1768	0.6356
LTHA	0.0664	0.3743	0.9706
RTHA	0.1362	0.1894	0.2665
LCER	0.2251	0.3352	0.1123
RCER	0.9989	0.3640	0.3546
LM1	0.1633	0.7927	0.7630
RM1	0.4530	0.9594	0.1533
LSMA	0.3840	0.2178	0.3488
RSMA	0.0756	0.3450	0.0645
LPFC	0.0768	0.6766	0.9222
RPFC	0.6469	0.3355	0.6124
LACC	0.2839	0.5993	0.1811
RACC	0.2551	0.5231	0.5781

Figure 5.

Analysis of potential practice and fatigue effects in brain activity. (**a**) Histogram of the differences between J_1 generated from the first and second halves of the voxel intensity time courses. All differences in J_1 across subject groups and ROIs were pooled in the histogram. Majority of the subjects showed minute difference in J_1. (**b**) *P* values obtained by applying a paired *t* test to J_1 generated from the first and second halves of the voxel intensity time courses separately for each group and ROI. No significant practice or fatigue effects were found for a liberal uncorrected threshold of $P < 0.05$. [Color figure can be viewed in the online issue, which is available at www.interscience.wiley.com.]

extent upon L-dopa administration, it is unlikely that practice effects contributed to our results. In addition, examination of error rates demonstrated that no significant differences in performance error between PD subjects off and on mediation were present, which suggests that repetition of the task in the on state did not lead to significant improvement in task performance. Moreover, comparing the spatial variance estimated from the first and second halves of the voxel intensity time courses did not detect any significant effects of practice or fatigue within a session (see Fig. 5). Hence, given over an hour of rest between sessions, fatigue is unlikely to have contributed to the detected activation changes, although this does not preclude potential motor consolidation between sessions. We note that ordering effects may be controlled by counterbalancing the scanning order of PD subjects. However, due to the washout period of L-dopa, counterbalancing would necessitate the on and off scans to be conducted on different days. Prior studies on the reproducibility of fMRI have demonstrated that when subjects perform an identical task on separate scanning sessions, the extent of activation could vary substantially [Bosnell et al., 2008; Marshall et al., 2004]. Hence, considering that spatial changes are the primary focus of this study, we opted to complete both scans on the same day.

Clinically, the finding of increased spatial distribution of activity in the primary motor cortex of PD subjects off medication is particularly interesting as it may help explain symptom progression in PD. Since the basal ganglia and its cortical loops are arranged somatotopically in a pattern from the feet to the face, a spread of activation related to movement of a specific part of the body may also lead to impaired movement in additional areas of the body. Recently, studies have shown that individuals whose symptoms start in the legs move first to the arms and body before moving to the head, neck, and face, while those whose first symptoms are in the arms are likely to see spread to both the lower body and head at a similar time [Dickson and Grunewald, 2004]. Our results would fit with this finding, suggesting that activity spreads from a focal area to a more diffuse pattern, slowly encompassing areas that normally control adjacent body parts.

In this article, using a novel method to quantify the spatial distribution changes in ROI activation, we demonstrated that L-dopa induces a similar focusing effect during motor tasks as that seen in cognitive studies. Our results suggest that spatial changes may be a robust feature of cortical and subcortical circuits for various types of behavior. In addition, we showed that incorporating spatial information enhances sensitivity in discriminating activation changes. Results in this study provided further support that one of the system-level effects of L-dopa may be the "refocusing" of activity in a broad range of cortical and subcortical structures. Thus, future fMRI studies investigating medication effects in PD should also consider spatial effects in addition to amplitude effects.

ACKNOWLEDGMENTS

This work was supported by an NSERC doctoral award and a Michael Smith Foundation award to Bernard Ng, a Canadian Institute of Health Research Canada Graduate Scholarship/Doctoral Research award to Samantha Palmer, and a Collaborative Health Research Project award to Martin J. McKeown and Rafeef Abugharbieh.

REFERENCES

Bosnell R, Wegner C, Kincses ZT, Korteweg T, Agosta F, Ciccarelli O, De Stefano N, Gass A, Hirsch J, Johansen-Berg H, Kappos L, Barkhof F, Mancini L, Manfredonia F, Marino S, Miller DH, Montalban X, Palace J, Rocca M, Enzinger C, Ropele S, Rovira A, Smith S, Thompson A, Thornton J, Yousry T, Whitcher B, Filippi M, Matthews PM (2008): Reproducibility of fMRI in the clinical setting: Implications for trial designs. Neuroimage 42: 603–610.

Brainard DH (1997): The psychophysics toolbox. Spat Vis 10: 433–436.

Buhmann C, Glauche V, Stürenburg HJ, Oechsner M, Weiller C, Büchel C (2003): Pharmacologically modulated fMRI—Cortical responsiveness to levodopa in drug-naive hemiparkinsonian patients. Brain 126: 451–461.

Castanon AN, Ghosh SS, Tourville JA, Guenther FH (2003): Region-of-interest based analysis of functional imaging data. NeuroImage 19: 1303–1316.

Cools R, Stefanova E, Barker RA, Robbins TW, Owen AM (2002): Dopaminergic modulation of high-level cognition in parkinson's disease: The role of the prefrontal cortex revealed by PET. Brain 125: 584–594.

Dickson JM, Grünewald RA (2004): Somatic symptom progression in idiopathic Parkinson's disease. Parkinsonism Relat Disord 10: 487–492.

Eidelberg D, Moeller JR, Dhawan V, Spetsieris P, Takikawa S, Ishikawa T, Chaly T, Robeson W, Margouleff D, Przedborski S, Fahn S (1994): The metabolic topography of parkinsonism. J Cereb Blood Flow Metab 14: 783–801.

Eidelberg D, Moeller JR, Kazumata K, Antonini A, Sterio D, Dhawan V, Spetsieris P, Alterman R, Kelly PJ, Dogali M, Fazzini E, Beric A (1997): Metabolic correlates of pallidal neuronal activity in Parkinson's disease. Brain 120: 1315–1324.

Feigin A, Fukuda M, Dhawan V, Przedborski S, Jackson-Lewis V, Mentis MJ, Moeller JR, Eidelberg D (2001): Metabolic correlates of levodopa response in Parkinson's disease. Neurology 57: 2083–2088.

Goodall C (1991): Procrustes methods in the statistical analysis of shape. J R Statist Soc B 53: 285–339.

Haslinger B, Erhard P, Kämpfe N, Boecker H, Rummeny E, Schwaiger M, Conrad B, Ceballos-Baumann AO (2001): Event-related functional magnetic resonance imaging in Parkinson's disease before and after levodopa. Brain 124 (Part 3):558–570.

Hoehn MM, Yahr MD (1967): Parkinsonism: Onset, progression and mortality. Neurology 17: 427–442.

Karni A, Meyer G, Jezzard P, Adams MM, Turner R, Ungerleider LG (1995): Functional MRI evidence for adult motor cortex plasticity during motor skill learning. Nature 377: 155–158.

Li SC, Sikström S (2002): Integrative neurocomputational perspectives on cognitive aging, neuromodulation, and representation. Neurosci Biobehav Rev 26: 795–808.

Liao R, Krolik JL, McKeown MJ (2005): An information-theoretic criterion for intrasubject alignment of FMRI time series: Motion corrected independent component analysis. IEEE Trans Med Imaging 24: 29–44.

Liu GT, Miki A, Goldsmith Z, van Erp TG, Francis E, Quinn GE, Modestino EJ, Bonhomme GR, Haselgrove JC (2002): Eye dominance in the visual cortex using functional MRI at 1.5 T: An alternative method. J AAPOS 6: 40–48.

Mattay VS, Tessitore A, Callicott JH, Bertolino A, Goldberg TE, Chase TN, Hyde TM, Weinberger DR (2002): Dopaminergic modulation of cortical function in patients with parkinson's disease. Ann Neurol 51: 156–164.

Marshall I, Simonotto E, Deary IJ, Maclullich A, Ebmeier KP, Rose EJ, Wardlaw JM, Goddard N, Chappell FM (2004): Repeatability of motor and working-memory tasks in healthy older volunteers: Assessment at functional MR Imaging. Radiology 233: 868–877.

McKeown MJ (2000): Detection of consistently task-related activations in fMRI data with hybrid independent component analysis (HYBICA). NeuroImage 11: 24–35.

Mehta M, Owen AM, Sahakian BJ, Mavaddat N, Pickard JD, Robbins TW (2000): Ritalin and working memory modulation in humans: Ritalin enhances working memory by modulating discrete frontal and parietal lobe regions in the human brain. J Neurosci 20: RC1–RC6.

Monchi O, Petrides M, Doyon J, Postuma RB, Worsley K, Dagher A (2004): The neural bases of set-shifting deficits in parkinsons disease. J Neurosci 24: 702–710.

Ng B, Abugharbieh R, Huang X, McKeown MJ (2006): Characterizing fMRI activations within regions of interest (ROIs) using 3D moment invariants. In Proc of IEEE Workshop on Mathematical Methods in Biomedical Image Analysis, New York, NY.

Ng B, Abugharbieh R, Huang X, McKeown MJ (2009): Spatial characterization of fMRI activation maps using invariant 3D moment descriptors. IEEE Trans Med Imaging 28: 261–268.

Playford ED, Jenkins IH, Passingham RE, Nutt J, Frackowiak RS, Brooks DJ (1992): Impaired mesial frontal and putamen activation in Parkinson's disease: A positron emission tomography study. Ann Neurol 32: 151–161.

Rorden C, Brett M (2000): Stereotaxic display of brain lesions. Behav Neurol 12: 191–200.

Rougemont D, Baron JC, Collard P, Bustany P, Comar D, Agid Y (1984): Local cerebral glucose utilisation in treated and untreated patients with Parkinson's disease. J Neurol Neurosurg Psychiatry 47: 824–830.

Sabatini U, Boulanouar K, Fabre N, Martin F, Carel C, Colonnese C, Bozzao L, Berry I, Montastruc JL, Chollet F, Rascol O (2000): Cortical motor reorganization in akinetic patients with Parkinson's disease: A functional MRI study. Brain 123: 394–403.

Sikstrom S (2007): Computational perspectives on neuromodulation of aging. Acta Neurochir Suppl 97 (Part 2):513–518.

Strafella AP, Ko JH, Grant J, Fraraccio M, Monchi O (2005): Corticostriatal functional interactions in Parkinson's disease: A rTMS/[11C]raclopride PET study. Eur J Neurosci 22: 2946–2952.

Talairach J, Tournoux M (1988): Co-Planar Stereotaxic Atlas of the Human Brain. New York: Thieme Medical Publishers.

Thickbroom GW, Phillips BA, Morris I, Byrnes ML, Mastaglia FL (1998): Isomteric force-related activity in sensorimotor cortex measured with functional MRI. Exp Brain Res 121: 59–64.

Turner RS, Grafton ST, McIntosh AR, DeLong MR, Hoffman JM (2003): The functional anatomy of parkinsonian bradykinesia. Neuroimage 19: 163–179.

Winterer G, Musso F, Vucurevic G, Stoeter P, Konrad A, Seker B, Gallinat J, Dahmen N, Weinberger DR (2006): COMT genotype predicts BOLD signal and noise characteristics in prefrontal circuits. Neuroimage 32: 1722–1732.

APPENDIX

Computation of 3D Moment Invariants

In this study, we are interested in examining the spatial extent of activation within each ROI to analyze the effects of L-dopa and movement frequency. The 3D moment invariant that measures such property is calculated as follows:

For a given ROI, we first scale the spatial coordinates (x,y,z) to account for ROI size differences across subjects [Goodall, 1991]:

$$x_s = x/s,\ y_s = y/s,\ z_s = z/s,$$
$$s = \sqrt{\sum_{i \in \mathrm{ROI}} ((x_i - \bar{x})^2 + (y_i - \bar{y})^2 + (z_i - \bar{z})^2)} \quad (1)$$

where $\bar{x}$, $\bar{y}$, and $\bar{z}$ are the centroid coordinates of the ROI and (x_s,y_s,z_s) are the scaled spatial coordinates. Summing centralized 3D moments, μ_{pqr}, as shown below results in a 3D moment invariant that measures spatial extent [Ng et al., 2006, 2009]:

$$J_1 = \mu_{200} + \mu_{020} + \mu_{002} \quad (2)$$

$$\mu_{pqq} = \iiint_{\mathrm{ROI}} (x_s - \bar{x}_s)^p (y_s - \bar{y}_s)^q (z_s - \bar{z}_s)^r \rho(x_s, y_s, z_s) dx_s dy_s dz_s \quad (3)$$

where $n = p + q + r$ is the order of the centralized 3D moment, μ_{pqr}, $\rho(x_s,y_s,z_s)$ is the t value of a voxel located at (x_s,y_s,z_s), and $\bar{x}_s$, $\bar{y}_s$, and $\bar{z}_s$ are the centroid coordinates of $\rho(x_s,y_s,z_s)$. Only positive t values are used in this study due to the presently unclear interpretation of negative t values, and the t values are normalized to the range of [0,1] to decouple the effects of amplitude from spatial changes [Ng et al., 2009]. The resulting spatial feature, J_1, is invariant to scaling (1), rotation (2), and translation (3), which accounts for differences in ROI sizes and subject's orientation in the scanner.